The Analysis and Design of a Dual-Band Self-Oscillating Mixer

Alishir Moradi Kordalivand[1], Sepideh Ebrahimi[2]
1- Young Researchers Club, Arak Branch, Islamic Azad University, Arak, Iran.
Email: alimoradi2020@gmail.com
2- Young Researchers Club,Islamic Azad University, Aligodarz Branch, Aligodarz, Iran.
Email: sepideh.ebrahimi87@yahoo

ABSTRACT:
Here, a self-oscillating mixer is experimentally demonstrated employing both the fundamental and harmonic signals generated by the oscillator sub-circuit in the mixing process. The resulting circuit is a dual-band down-converting mixer that can operate in the C-band, or in the X-band. The oscillator uses the active super harmonic coupling to enforce the quadrature relationship of the fundamental outputs. Either the fundamental outputs of the oscillator or the second harmonic oscillator output signals present at the common mode nodes are connected to the mixer via a set of complementary switches. The mixer achieves a conversion gain between 9–11.5 dB in both frequency bands. The third-order output intercept-point for the C-band and the X–band operations are 10.42 and 8.33 dBm, respectively. The circuit was designed and simulated in 0.18- CMOS technology by ADS2008.

1. INTRODUCTION

In modern microwave communication systems, low cost, small size, and low power consumption circuits are required that combine multiple functions with a reduced number of components. For the realization of receiving systems, the harmonic self-oscillating mixer (SOM) is an attractive option [1]–[6], since a single transistor is employed to realize the local oscillator signal as well as a mixing operation between the input signal and a harmonic component of the self-oscillation. In harmonic balance (HB), several techniques have been presented for the nonlinear analysis and design of SOM-circuits [5], [6]. With these techniques, the designer has an increased control over the SOM self-oscillating frequency, the harmonic content, and the conversion gain. However, for the design of wide-band harmonic SOM circuits with high conversion gain, additional techniques are required.

A common problem referring to SOM solutions has been the Lack RF-to-local oscillator (LO) isolation emerging by the combination of the two circuit functions into one device. This problem has been addressed in numerous publications, and a common solution to bypass this issue is given using a dual-gate FET, using one port for the oscillation feedback network and injecting the RF input signal at the second port [7]–[9]. Another possibility to eliminate this problem is the use of a balanced circuit structure [10]–[13], which offers inherent RF-LO isolation, as well as

a number of other important advantages such as lower AM noise, suppression of unwanted harmonics, etc. Furthermore, the input does not have to be matched both at LO and RF frequencies, which simplifies the input matching requirements.

Efforts have been made to integrate SOMs with antennas to form receivers [7], [9], [14]. This allows for building a simple receiver circuit without the use of an input RF balun, as it would be required in conventional balanced mixers. Thus, the presented solution results in a planar design, which is highly desired in many commercial low-cost applications.

An extension to the standard SOM technique is subharmonic operation [8]–[11], [15]: instead of mixing the RF signal with the fundamental LO frequency, a harmonic of the LO frequency is used. In this way, transistor gain only has to occur until the fundamental LO frequency, which drastically lowers the transistor maximum frequency (f_{max}) requirements [15].

The paper is structured as follows: Section 2 describes Block diagram of the proposed dual-band Self-Oscillating Mixer (SOM); Section 3 presents design Quadrature VCO and simulation result with Agilent's Advanced Design System ADS; and Section 4 discusses the subhormonic and fundamental mixer design; and section 5 discusses mixer simulation results obtained with ADS.

2. CIRCUIT DESCRIPTION

Block diagram of the proposed dual-band SOM is shown in Fig. 1. This figure shows a down converting mixer with differential RF input and IF output, as well as a reconfigurable LO input.

If an LO is available that has a differential output at both f_{LO} and $2f_{LO}$ two pairs of complementary switches can be used to connect the desired LO signal to the mixer. Depending on the state of the switches, the mixer can have an LO input in two different frequency bands, thus permitting two different RF frequency bands at the mixer input while maintaining a constant IF output. The result is a dual-band SOM using a single on-chip quadrature voltage-controlled oscillator (VCO) along with a single mixer circuit. To distinguish between the two states of the dual-band SOM, the term "fundamental mode" will be used to describe the circuit state where the fundamental oscillator output at f_{LO} is connected to the mixer, and the term "subharmonic mode" will be used to describe the state where the $2f_{LO}$ signal is connected to the mixer.
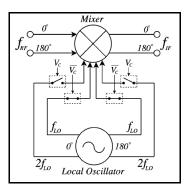

Fig. 1. Block diagram of the proposed dual-band SOM.

The core of the subharmonic mixer is shown in figure2, which is based on the Gilbert-cell topology. Gilbert-cell mixers, in general, have high isolation between Ports due to their double-balanced structure. Corresponding to the block diagram in Figure1, the circuit requires RF inputs with relative phase shifts of 0°, and 180°, and LO inputs of 0°, 90°, 180°, and 270° [16] .

For insight into how the LO frequency is doubled, consider the circuit in Figure3. As the 0° LO signal rises well above the threshold value, transistor M5 turns fully on, causing i_1 to increase and flow predominately through M5, since the gate voltage at M6 is 180° out of phase and therefore, near its minimum. When the amplitude of the 0° LO signal begins to drop, and the 180° LO amplitude begins to rise, neither transistor is fully on and, as a result, the current i_1 decreases. As the 180° LO signal nears its maximum, and the 0° LO nears its minimum, M6 is turned fully on and M5 is turned off, meaning that the current i_1 increases and flows through M6. By the end

of the cycle, neither the 0° nor the 180° LO signals are at a maximum and the current i_1 decreases again. Therefore, during one period of the LO signal, i_1 has two cycles of increasing and decreasing current, thus indicating a doubling of the LO frequency.

The same operation occurs for the other LO transistor pair (90° and 270°) and the resulting current, i_2, is 180° out of phase with i_1.
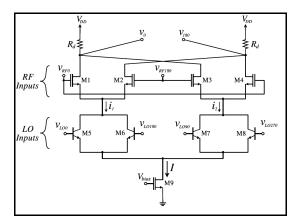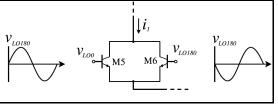

Fig. 2. Proposed CMOS 2× subharmonic mixer core.

Fig. 3. LO frequency doubling in the 2× subharmonic mixer

Therefore, mixing will occur at the RF frequency and twice the input LO frequency. A larger LO input power will be required to achieve the same conversion gain as a fundamental Gilbert-cell mixer, but this circuit has the significant advantage of using half of the LO frequency as well as reducing LO self-mixing in direct-conversion receivers .

The LO inputs to the subharmonic mixer are given by:

$$v_{LO0} = A_{LO}\cos(\omega_{LO}t)$$

$$v_{LO90} = A_{LO}\cos(\omega_{LO}t - \pi/2)$$

$$v_{LO180} = A_{LO}\cos(\omega_{LO}t - \pi)$$

$$v_{LO270} = A_{LO}\cos(\omega_{LO}t - 3\pi/2)$$

and the RF inputs to the mixer core are differential,

$$v_{RF0} = A_{RF}\cos(\omega_{RF}t)$$

$$v_{RF180} = A_{RF}\cos(\omega_{RF}t - \pi)$$

since this is a 2× SHM, the up- and down-converted components of the mixer output will be at $f_{RF} + 2f_{LO}$

and f_{RF} - $2f_{LO}$, respectively.

To gain deeper insight into the operation of the SHM, an analytic expression for the conversion gain of the mixer can be derived. Here, the long-channel transistor models are used for simplicity in order to obtain useful closed-form equations. In the half-SHM circuit shown in Figure 4, the LO switching pair transistors M5-M6 is modeled as one transistor, M56. Assuming that the fundamental currents generated by the differential gate voltage signals on M5 and M6 perfectly cancel each other, the non-linear component at twice the input frequency is the only signal current that remains. Therefore, M5 and M6 are modeled as one transistor with an applied gate voltage signal at a frequency of 2ωLO. Transistors M7 and M8 in Figure 2 can also be replaced by a single equivalent transistor M78. The long channel drain current approximation for a FET in saturation is given by:

$$i_D = \frac{1}{2}\mu_n C_{ox}\frac{W}{L}(v_{GS}-V_t)^2 \qquad (1)$$

where μ_n is the electron mobility, C_{ox} is the gate capacitance, v_{GS} is the gate-source voltage, and V_t is the threshold voltage.

And for BJT given by:

$$i_e = \frac{1}{2}\mu_n C_{oy}\frac{W}{L}(v_{BE}-V_t)^2 \qquad (2)$$

where μ_n is the electron mobility, C_{oy} is the Base capacitance, v_{BE} is the Base-Emitter voltage, and V_t is the threshold voltage.
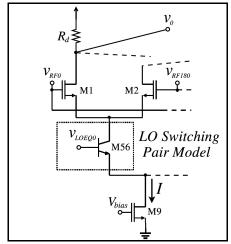

Fig. 4. Modeling of the LO switching transistors as one FET with input v_{LOEQ0}.

If the currents through M5 and M6 are i_a and i_b, respectively, the total current from the switching pair with a differential input is:

$$i_1 = i_a + i_b = \mu_n C_{oy}\frac{W_1}{L}(V_{BE(LO)}-V_t)^2 + \frac{1}{2}\mu_n C_{oy}\frac{W_1}{L}(V_{LO0}^2 - V_{LO180}^2) \qquad (3)$$

where $V_{BE(LO)}$ is the DC voltage between the Base and Emitter of the LO transistors (M5-M8). Since $v_{LO0}^2 = v_{LO180}^2$ for a sinusoidal LO signal,

$$i_1 = \mu_n C_{oy}\frac{W_1}{L}(V_{BE(LO)}-V_t)^2 + \mu_n C_{oy}\frac{W_1}{L}V_{LO0}^2 \qquad (4)$$

This current can then be set equal to the current generated by the M56 model transistor (ignoring the nonlinear component),

$$i_1 = \frac{1}{2}\mu_n C_{oy}\frac{W_2}{L}(v_{BE(LO)}-v_t)^2 + \mu_n C_{oy}\frac{W_2}{L}(v_{BE(LO)}-V_t)v_{LOEQ0} \qquad (5)$$

Clearly, in order to have equal DC currents, the width of transistor M56 must be twice that of M5 and M6, $W_2=2W_1$. The equivalent applied gate signal voltages to the LO switching pair model transistors, M56 and M78, are:

$$v_{LOEQ0} = \frac{A_{LO}^2}{2(V_{BE(LO)}-V_t)}\cos^2(\omega_{LO}t) \approx \frac{A_{LO}^2}{4(V_{BE(LO)}-V_t)}\cos(2\omega_{LO}t) \qquad (6)$$

$$v_{LOEQ180} = \frac{A_{LO}^2}{2(V_{BE(LO)}-V_t)}\cos^2(\omega_{LO}t+\pi) \approx \frac{A_{LO}^2}{4(V_{BE(LO)}-V_t)}\cos(2\omega_{LO}t+\pi) \qquad (7)$$

The approximation made in the equations (6) and (7) was to ignore the DC component of the $\cos^2$ term, the effect of which will be discussed below. With this simplification, the circuit can be analyzed as a standard Gilbert-cell topology, with the addition of the injection resistors. The output voltage of the mixer, $v_{OUT}=v_0 - v_{180}$, as defined in Figure 2, is given by:

$$v_{OUT} = \frac{-R_d v_{idRF}}{V_{GS(RF)}-V_t}(i_1-i_2) = \frac{-R_d I}{(V_{GS(RF)}-V_t)(V_{GS(LO)}-V_t)}v_{idRF}v_{idLOEQ} \qquad (8)$$

Where $v_{idRF}=v_{RF0}-v_{RF180}$, $v_{idLOEQ}=v_{LOEQ0}-v_{LOEQ180}$, and $V_{GS(RF)}$ is the DC voltage between the gates and sources of the RF transistors (M1-M4).

The conversion gain formula for this subharmonic mixer for the up- and down- converted components ($f_{RF}+2f_{LO}$ and $f_{RF}-2f_{LO}$) is given by:

$$CG_{dB} = 20\log\left(\frac{R_d I A_{LO}^2}{4(V_{GS(RF)}-V_t)(V_{BE(LO)}-V_t)^2}\right) \qquad (9)$$

where I is the bias current set by the gate voltage of transistor M9, A_{LO} is the amplitude of the quadrature signal at the gates of the LO transistors M5-M8, and all transistors are operating in the saturation region. The values for $V_{GS(RF)}$ and $V_{BE(LO)}$ can be found from a straight-forward DC circuit analysis. From this equation, clearly the conversion gain will increase with increasing bias current, I.

The formula for the conversion gain in (9) does not include the effects of any parasitic, and thus, it will over-estimate the actual conversion gain. However, the simplification in Equations (6) and (7) where the DC component of the $\cos^2$ term was not included mitigates the over-estimation in (9) somewhat since there is an additional DC component in the currents that are generated by M5-M8 (or M56 and M78).

3. PROPOSED QUADRATURE VCO

A very common way of implementing a CMOS differential LC VCO is to use a cross-coupled pair to generate the negative resistance required to overcome the losses in the tank. Therefore, with an appropriate device size and biasing, the negative resistance required to counteract the losses in the tank can be realized. The core quadrature VCO circuit investigated in this work is shown in Figure 3. It consists of two cross-coupled VCO connected through a cross coupled pair. It has been shown that by including cross-coupled inductor above the cross-coupled NPN transistors the phase noise of the VCO can be improved significantly due to the higher transconductance and faster switching speed of the complementary structure [11]. The oscillation frequency for each VCO can be found from the familiar formula for the resonant frequency of an LC tank, where L is the value of the on-chip spiral inductor and C is the total capacitance at the tank nodes. The inductors used in this circuit less than 1.1nH. The total capacitance including the lumped capacitor as well as the parasitic capacitance was 0.925pF to provide oscillation at 4.8GHz.

The network used to enforce the 180° phase difference in the second-order harmonics is a critical part of the quadrature VCO. It is this anti-phase relationship that creates the quadrature phase relationship at the fundamental frequency. Convenient common-mode nodes for coupling the second harmonic are the common source nodes in each of the cross-coupled differential pairs, shown as CM1 and CM2 in the complete VCO circuit schematic shown in Figure 2. DC blocking capacitors were used so that transistors N5-N6 could be biased for optimal coupling. Since any practical use of a VCO involves connecting its output to other circuitry, buffers must be used to ensure that loading does not disrupt the oscillations. Source follower buffers were used for each of the four outputs so that the VCO can be measured using equipment with

$50\,\Omega$ input impedances. The current sources shown in the buffer circuits in Figure 2 were implemented with the common current-mirror configuration. t. The 180° and 270° outputs were terminated on-chip with $50\,\Omega$ loads and the 0° and 90° were connected to CPW pads for on-chip probing.
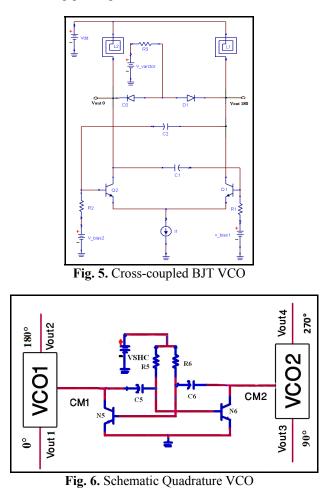

Fig. 5. Cross-coupled BJT VCO

Fig. 6. Schematic Quadrature VCO

Table 1 shows result of fundamental (4.8GHz) and subharmonic (9.6GHz) VCO.

Table 1. Result of fundamental and subharmonic VCO.

	Fundamental	Subharmonic
Freq	4.8GHz	9.6GHz
Output Power	-0.942dBm	-9.751dBm
Phase Noise	-107.2 dBc/Hz	-111.8 dBc/Hz

4. MIXER

The mixer circuit uses the top half of the traditional Gilbertcell topology. Fig. 4 shows a simplified circuit schematic of the mixer in the subharmonic mode. The common-mode node where the second harmonic signal

is dominant is connected to the sources of the RF transistors.

These $2f_{LO}$ signals at CM1 and CM2 are 180 out of phase with each other, which maintains the double-balanced characteristic of the Gilbert cell. The circuit could be implemented as shown in Fig. 4 as a single-band mixer with the doubled LO frequency output. If implemented in this way, the use of an additional frequency doubler circuit connected to the fundamental output could be avoided, thus saving chip space and reducing power consumption.
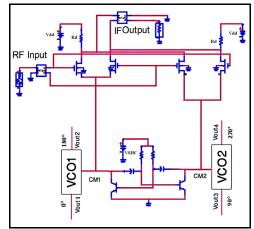

Fig. 7. Simplified circuit of the proposed dual-band SOM in subharmonic mode.

A simplified circuit diagram of the dual-band SOM is shown in Fig. 5. Included in this figure are the four source–follower buffers that are connected to the fundamental quadrature oscillator output. The value of R_b was selected to equalize the fundamental signal amplitude with the $2f_{LO}$ signal amplitude at CM1 and CM2. To select the fundamental mode for the mixer, the control voltage V_C is set to V_{dd}, turning on switches SW1 and SW2 and turning off switches SW3 and SW4. This connects the 0° and 180° fundamental outputs at f_{LO} to the sources of the RF transistors. The 90° and 270° fundamental outputs are connected to identical source–follower buffers as the 0° and 180° outputs to maintain equal loads to the oscillator tank.

Note that the 90° and 270° fundamental outputs of the oscillator are not used in the fundamental mode of operation; however, they are required to generate the $2f_{LO}$ signal at CM2 for the subharmonic mode, and they could be used elsewhere in the system if needed. For the subharmonic mode, the control voltage V_C=0 V, turning off switches SW1 and SW2, and turning on switches SW3 and SW4. This connects the 0° and 180° degree $2f_{LO}$ signals to the sources of the RF transistors.

Each of the two outputs of the mixer at V_{IF+} and V_{IF-} are connected to source–follower buffers and connected to bonding pads. These two signals are combined off-chip and connected to the 50-

measurement equipment. The 50Ω source–follower buffers and combiner were designed such that the output voltage amplitude across the load of the measurement equipment is equal to (V_{IF+} - V_{IF-}).
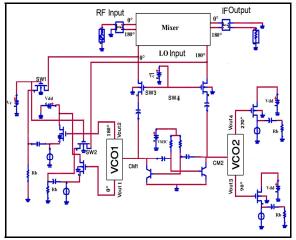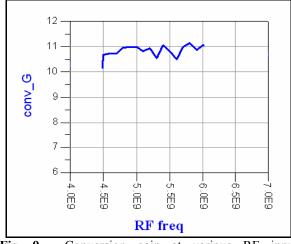

Fig. 8. Circuit of the proposed dual-band SOM.

Alternative circuit configurations are possible to achieve a similar behavior to that presented in this study. For example, an oscillator whose fundamental frequency is $2f_{LO}$ followed by a frequency divider to generate the f_{LO} signal could be used. While the quadrature oscillator approach employed here does lead to a certain overhead in dc power dissipation due to the need for two oscillators, using the frequency-divider method would not necessarily bring significant savings in dc power since frequency dividers can easily consume as much power as a single oscillator. Another possible configuration is to only use the fundamental outputs of the quadrature oscillator along with the subharmonic mixer described in [16] and [17]. In that type of subharmonic mixer, the four transistors in the LO path require quadrature inputs at 0°, 90°, 180°, and 270°, which is precisely what the quadrature oscillator provides. In order to achieve dual-band operation, a series of switches is needed to connect the 0°, 90°, 180°, and 270°, signals to the appropriate LO transistors for the subharmonic mode, and only connect the 0° and 180° to the appropriate LO transistors for the fundamental mode. It was found through simulation that greater conversion gain could be achieved by directly using the doubled frequency component already present at the common mode in contrast to using the quadrature fundamental outputs with an LO doubling pair. Furthermore, a lower noise figure was obtained by using the $2f_{LO}$ signal directly from the oscillator due to the elimination of the switching noise that accompanies the LO doubling pairs in the subharmonic mixer topology of [16] and [17].

5. SIMULATION RESULTS
5.1. Fundamental Results

Supply voltage V_{dd} was set to 1.8V. The conversion gain of the mixer was a measurement Fundamental states at various RF frequencies, and the results are shown in Fig. 6. An IF frequency of 200 MHz was used, giving an RF input frequency 5.0 GHz fundamental mode, respectively. Fig 7 shows noise figure in fundamental mode.

Fig. 9. Conversion gain at various RF input frequencies for a fixed IF frequency of 200 MHz. in fundamental mode
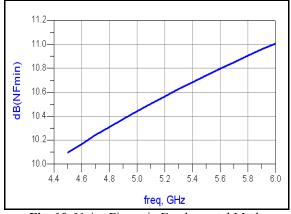

Fig. 10. Noise Figure in Fundamental Mode

5.2. Subharmonic Results

The conversion gain of the mixer was a measurement Fundamental states at various RF frequencies and the results are shown in Fig. 8. An IF frequency of 200 MHz was used, giving an RF input frequency 9.8 GHz fundamental mode, respectively. Fig 9 shows noise figure in fundamental Mode. Table 2. Shows Result of fundamental and subharmonic mixer.

Fig. 11. Conversion gain at various RF input frequencies for a fixed IF frequency of 200 MHz. in subharmonic Mode
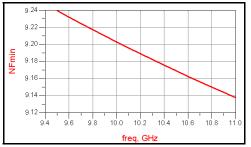

Fig. 12. Noise Figure. in Subharmonic Mode

Table 2. Resuat of fundamental and subharmonic Mixer.

	Fundamental	Subharmonic
Conv_gain(dB)	10.5-11.2	9-11.3
Noise Figure(dB)	10.1-11	9.13-9.23
IIP3	10.42	8.33
Isolation RF2IF(dB)	40	45

6. CONCLUSION

A new topology for a dual-band SOM has been demonstrated using CMOS 0.18 μm technology. This technique uses both the fundamental and second harmonic outputs of a single on-chip quadrature VCO connected to a mixer through complementary switches. For C-band operation, switches connect the fundamental oscillator output to the mixer, and for X-band operation, switches connect the second harmonic of the oscillator to the mixer. The mixer achieves a conversion gain of at least 9 dB over RF frequencies of 5.0 to 6.0 GHz and from 9.8 to 11.8 GHz while maintaining a constant IF output. This circuit could be used as part of a multistandard system on a chip to reduce the number of circuit elements required, potentially resulting in lower power consumption and reduced costs. This technique could also be very attractive to millimeter-wave frequencies where the use of a frequency-doubler circuit connected to the output of an LO could be avoided, and in cases where the use of a broadband mixer circuit is not possible.

REFERENCES

[1] G. C. Wang *et al.*, **"A low cost DBS low noise block downconverter with a DR stabilized MESFET self-oscillating mixer,"** in *IEEE MTT-S International Digest*, May 1994, vol. 3, pp. 1447–1450.

[2] M.-R. Tofighi and A. S. Daryoush, **"A 2.5-GHz InGaP/GaAs differential cross-coupled Self-Oscillating Mixer (SOM) IC,"** *IEEE Microwave.Wireless Components Letters*, vol. 15, no. 4, pp. 211–213, Apr. 2005.

[3] S. A. Winkler, K. Wu, and A. Stelzer, **"Integrated receiver based on a high-order subharmonic self-oscillating mixer"** *IEEE Trans. Microwave Theory Techniques*, vol. 55, no. 6, pp. 1398–1404, Jun. 2007.

[4] F. Plessas, A. Papalambrou, and G. Kalivas, **"A subharmonic injectionlocked self-oscillating mixer"** in *Proc. IEEE International Symposium Circuits and Systems*, New Orleans, LA, May 2007, pp. 2626–2629.

[5] S. Ver Hoeye, L. Zurdo, and A. Suárez, **"New nonlinear design tools for self-oscillating mixers"** *IEEE Microwave.Wireless Components Letters*, vol. 11, no. 8, pp. 337–339, Aug. 2001.

[6] L. F. Herrán, S. Ver Hoeye, and F. Las Heras, **"Nonlinear optimization tools for the design of microwave high-conversion gain harmonic selfoscillating mixers"** *IEEE Microwave.Wireless Components Letters*, vol. 16, no. 1, pp. 16–18, Jan. 2006.

[7] J. Zhang, Y.Wang, and Z. Chen, **"Integration of a self-oscillating mixer and an active antenna"** *IEEE Microwave.Wireless Components Letters*, vol. 9, no. 3, pp. 117–119, Mar. 1999.

[8] J. Xu and K.Wu, **"A subharmonic self-oscillating mixer using substrate integrated waveguide cavity for millimeter-wave application"** in *IEEE MTT-S International Microwave Symposium Digest*, Jun. 2005, pp. 2019–2022.

[9] Y. Chen and Z. Chen, **"A dual-gate FET subharmonic injection-locked self-oscillating active integrated antenna for RF transmission"** *IEEE Microwave.Wireless Components Letters*, vol. 13, no. 6, pp. 199–201, Jun. 2003.

[10] S. A. Winkler, K. Wu, and A. Stelzer, **"A novel balanced third and fourth harmonic self-oscillating mixer with high conversion gain"** in *Proc. 36th European Microwave Conference*, Manchester, U.K., Sep. 2006, pp. 1663–1666.

[11] M. Sironen, Y. Qian, and T. Itoh, **"A subharmonic self-oscillating mixer with integrated antenna for 60-GHz wireless applications"** *IEEE Trans. Microwave Theory Techniques*, vol. 49, no. 3, pp. 442–450, Mar. 2001.

[12] N. Siripon, K. S. Ang, M. Chongcheawchamnan, and I. D. Robertson, **"Design and performance of a novel balanced self-oscillating mixer"** in *Proc. 30th European Microwave Conference*, Paris, France, Oct. 2000, pp. 16–19.

[13] N. Bourhill, S. Iezekiel, and D. P. Steenson, **"A balanced self-oscillating mixer"** *IEEE Microwave Guided Wave Lett.*, vol. 10, no. 11, pp. 481–483, Nov. 2000.

[14] T.-C. Huang and S.-J. Chung, **"A new balanced self-oscillating mixer (SOM) with integrated antenna"** in *IEEE Int. AP-S Symposium*, Columbus, OH, USA, Jun. 2003, pp. 89–92.

[15] D. H. Evans, **"A millimetre-wave self-oscillating mixer using a GaAs FET harmonic-mode oscillator"** in *IEEE MTT-S Int. Microwave Symposium Digest*, Jun. 1986, pp. 601–604.

[16] K. Nimmagadda and G. Rebeiz, **"A 1.9 GHz double-balanced subharmonic ixer for direct conversion receivers"** in *IEEE Radio Freqency Integrated Circuits Symposium, Digest*, 2001, pp. 253–256.

[17] B. R. Jackson and C. E. Saavedra, **"A CMOS subharmonic mixer with nput and output active baluns"** *Microwave Optical Technology Letters*, vol. 48, p. 2472–2478, Dec. 2006.